AIAA JOURNAL
Vol. 37, No. 10, October 1999

Green's Function Discretization Scheme for Sound Propagation in Nonuniform Flows

P. Di Francescantonio*
STS Scientific and Technical Software, 21020 Mornago (VA), Italy
and
D. Casalino†
Turin Polytechnic, 10129 Turin, Italy

A new frequency-domain discretization technique that permits the numerical solution of the equation governing the propagation of small disturbances within nonuniform potential flows is described. The method can be applied successfully to the numerical solution of aeroacoustic problems because a good accuracy is preserved up to 3–4 points per period for three-dimensional unstructured meshes. The discretization scheme is based on a local interpolation formula that is strictly joined to the physics of wave propagation because it is constructed with the superimposition of elementary sources that are local solutions of the local convective wave equation. The method presents aspects in common with both finite difference and finite element methods, with the peculiarity that the local interpolation formula can be interpreted as a specific shape function introduced to take advantage of the physics of the problem. The method is applied to the potential equation linearized around an arbitrary aerodynamic mean flow, and several comparisons with theoretical results, as well as several convergence tests, are conducted to show that a good accuracy is preserved up to 3–4 points per period also for irregular meshes with both random and systematic distortions. Numerical calculations are presented for three-dimensional problems with both uniform and nonuniform flow, and comparisons are made with theoretical and other available numerical results. With the appropriate generalizations, the method can be regarded as a new, efficient general approach for the discretization of generic partial differential equations.

Nomenclature

A^i_m = discretized Helmholtz operator for node i
c_∞ = sound velocity in the undisturbed fluid
G_c = convective Green's function,

$$G_c(\bar{r}_1, \bar{r}_2; \bar{M}_\infty) = \exp\left(\mathrm{i}\left(k/\beta_\infty^2\right)\left\{-(\bar{r}_1 - \bar{r}_2)\cdot\bar{M}_\infty + \sqrt{[(\bar{r}_1 - \bar{r}_2)\cdot\bar{M}_\infty]^2 + \beta_\infty^2|\bar{r}_1 - \bar{r}_2|^2}\right\}\right) \times \left\{[(\bar{r}_1 - \bar{r}_2)\cdot\bar{M}_\infty]^2 + \beta_\infty^2|\bar{r}_1 - \bar{r}_2|^2\right\}^{-0.5}$$

G_o = nonconvective Green's function (Helmholtz equation), $G_o(\boldsymbol{r}_1, \boldsymbol{r}_2) = e^{\mathrm{i}k|\boldsymbol{r}_1 - \boldsymbol{r}_2|}/|\boldsymbol{r}_1 - \boldsymbol{r}_2|$
G_{mn} = element m, n of matrix G, which expresses the influence of the nth source on the potential at the mth node of the stencil of i; $G_o(\boldsymbol{r}^p_m, \boldsymbol{r}^s_n)$
G^+_{nm} = element n, m of pseudoinverse of matrix G
i = imaginary unit $\sqrt{-1}$
i = index of ith nodes
k = wave number, ω/c_∞
$M(i)$ = number of nodes that constitute the computational molecule (or stencil) of node i
$\bar{\boldsymbol{M}}$ = local Mach vector of aerodynamic field, $\bar{U}/c_\infty$
$\bar{\boldsymbol{M}}_\infty$ = Mach vector of undisturbed flow, $\bar{U}_\infty/c_\infty$
N = number of fictitious sources
N_d = number of internal nodes
N_t = total number of nodes (internal + boundary)
$\boldsymbol{r}^p_m$ = position of mth node of the stencil
$\boldsymbol{r}^s_n$ = position of nth fictitious source
β^2_∞ = $1 - M^2_\infty$
γ_n = complex intensity of nth fictitious source
ϕ_i = complex potential at ith node
ϕ^i_m = complex potential at mth node of stencil of node i

Introduction

THE numerical simulation of sound generation and propagation by direct solution of aerodynamic field equations, usually known as computational aeroacoustics (CAA), has received more and more attention in the past few years from the scientific community. The reason for the growing interest is that CAA methods, in principle, can take into account all of the nonlinear effects. However, their application for realistic problems, in particular for three-dimensional cases, is limited by the great amount of computational resources required. Great research efforts are therefore devoted to this subject, and two major aspects are under investigation.[1] The first concerns an accurate implementation of boundary conditions to reduce the extension of the computational domain, and the second focuses on the development of specific discretization schemes to reduce the minimum number of points per wave. In three dimensions the total number of nodes is proportional to the third power of the number of points per wave, and so, the importance of any reduction even if small can be understood easily. Presently, two different approaches are applied in CAA, depending on the kind of problem to be addressed. If the acoustic disturbances strongly interact with the aerodynamic field or, in other words, if the acoustic quantities cannot be considered small compared to the aerodynamic ones, the full nonlinear equations have to be solved jointly for aerodynamics and acoustics. In the other case, when the acoustic disturbances are small, the full nonlinear equations still can be applied, but they may cause some problems because of the different order of magnitude of the steady aerodynamic quantities with respect to the unsteady acoustic disturbances. Sometimes, therefore, it is preferred to linearize around the mean aerodynamic flowfield and solve for the linear acoustic disturbance in the nonuniform mean flow. In this paper, the latter case is addressed, and a frequency-domain formulation is presented that substantially reduces the required number of discretization nodes. The central idea is based on the construction of a local interpolation formula that can be considered somehow to be connected to the nature of the wave propagation and that is used to derive the discretization scheme.

Received 22 December 1997; revision received 5 October 1998; accepted for publication 5 March 1999.

*Acoustic Specialist, Via C. Battisti 24; mc0477@mclink.it.
†Aeronautic Engineer, Corso duca degli Abruzzi 24.

In the proposed approach the local interpolation is constructed with the superimposition of simple sources that are local elementary solutions (Green's functions) of the local linear convective wave equation. The original idea was derived by Caruthers et al.,[2] who focused on the solution of the Helmholtz equation. In their work, Caruthers and colleagues build a local interpolation formula that automatically satisfies the Helmholtz equation and then searches for a solution that only satisfies the boundary conditions because the verification of the governing equation already is ensured. The major limitation of this approach is that it can be applied only in cases for which the Green's function of the governing equation is known[2,3] or when it reasonably can be computed in an approximate form.[4] In the present work, the field of applicability is enlarged greatly. A similar local interpolation formula in fact is adopted, but it is used to derive a differentiation scheme that is used to discretize the governing equation effectively. The philosophy of the method is therefore much closer to classical finite difference (FD) or finite element (FE) methods, with the peculiarity that the shape functions (the local interpolation formulas) are joined more closely to the nature of the problem to be solved.

The method is applied here to the discretization of the acoustic potential equation linearized around a generic aerodynamic mean flow. Accuracy and convergence tests conducted on three-dimensional test cases show that the method produces good results up to 3–4 points per period per dimension. Tests with randomly or systematically distorted grids also show that the accuracy of the method is not degraded unless very strong distortions are introduced.

The method is described first for the Helmholtz equation, and then the general case of a small-disturbance propagation in a nonhomogeneous medium is considered.

Numerical Method

The first step required to derive the new formulation is the construction of a local interpolation formula that permits efficient modeling of acoustic phenomena. The interpolation formula that we use was developed by Caruthers et al.,[2,3] and we adapt it to our discretization technique with a few modifications.

For simplicity, we consider a generic domain in which the Helmholtz equation is verified and suppose that we want to reconstruct the potential distribution $\phi(\boldsymbol{r})$ inside a small region V_M once the values of $\phi_m = \phi(\boldsymbol{r}_m^p)$ are defined for a certain number M of points $\boldsymbol{r}_m^p$ inside V_M (Fig. 1). A classical approach could be based on the construction of a triangularization among the M points and on the use of classical FE shape functions. With that procedure we obtain an interpolation formula that is independent of the governing equation, and therefore we cannot take any advantage from the knowledge of the properties of the Helmoholtz equation itself.

An alternative approach is to follow the work of Caruthers et al.[2,3] We can assume that the potential distribution inside V_M is produced by the superimposition of N fictitious simple sources, each of which satisfies the Helmholtz equation in such a way that their spatial distribution and intensity produce the given potential ϕ_m at the points $\boldsymbol{r}_m^p$. Clearly, a number of possibilities exist for the definition of the sources. Among them, a simple, efficient approach is to choose a priori the source positions (typically, uniformly distributed on a sphere surrounding the region V_M) and to assume that only their intensities are unknown. A linear system therefore can be obtained that relates the N unknown source intensities to the M known potential values. Clearly, a unique solution can exist only if $N = M$, and one therefore would think that having the number of sources equal to the number of points is mandatory. One key idea proposed by Caruthers et al.[2,3] is instead to use $N > M$ because it is reasonable to expect that increasing the number of sources improves the quality of the reconstruction. In fact, with $N = M$, we can obtain great oscillations within the region V_M because, the solution being unique, nothing assures us that the N sources do not present great oscillations in the intensity, and so the sources could produce the desired value of the potential at the points M by means of great cancellations that occur only at the positions of the M points. Therefore, some constraint must be imposed on the oscillations of the source intensity, and this can be done using $N > M$ and choosing from among the infinite solutions the one that minimizes the L^2 norm of the source intensities. Once the source intensities are known, the potential $\phi(\boldsymbol{r})$ in a generic point of V_M can be obtained by summing the contribution of the sources and in this way obtaining the desired interpolation formula. Following the nomenclature of Caruthers et al.,[2] we refer to the proposed method as the Green's function interpolation (GFI).

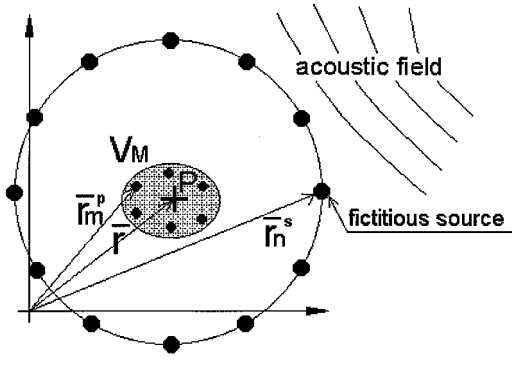

Fig. 1 Numerical method.

Interpolation Scheme

We now can go into deeper detail in the mathematical formalism of the above procedure. The complex acoustic velocity potential produced by the N fictitious sources in the generic point $\boldsymbol{r}$ is given by

$$\phi(\boldsymbol{r}) = \sum_{n=1}^{N} \gamma_n G_o(\boldsymbol{r}, \boldsymbol{r}_n^s) \tag{1}$$

Imposing the verification of relation (1) at each of the M points $\boldsymbol{r}_m^p$ where the value of the potential is known, we obtain

$$\phi(\boldsymbol{r}_m^p) = \phi_m = \sum_{n=1}^{N} \gamma_n G_o(\boldsymbol{r}_m^p, \boldsymbol{r}_n^s) = \sum_{n=1}^{N} \gamma_n G_{mn} \qquad (m = 1, M) \tag{2}$$

Equation (2) can be interpreted as a linear system of M complex equations with N unknowns γ_n. As already said, we consider the case $N > M$ and we impose a minimum L^2 norm constraint, selecting the solution for which

$$\sum_{n=1}^{N} \gamma_n^2$$

is minimum. This condition can be imposed indirectly by computing the pseudoinverse[5] matrix of $[G]$, which is indicated as $[G^+]$. The desired solution of Eq. (2) therefore can be written as

$$\gamma_n = \sum_{m=1}^{M} G_{nm}^+ \phi_m \qquad (n = 1, N) \tag{3}$$

Substituting Eq. (3) into Eq. (1) and commuting the sum operators, we obtain

$$\phi(\boldsymbol{r}) = \sum_{m=1}^{M} F_m(\boldsymbol{r}) \phi_m \tag{4}$$

where

$$F_m(\boldsymbol{r}) = \sum_{n=1}^{N} G_{nm}^+ G_o(\boldsymbol{r}, \boldsymbol{r}_n^s) \tag{5}$$

Equation (4) allows us to obtain the potential distribution at a generic point $\boldsymbol{r}$ of V_M once the potential ϕ_m is known for M generic points, and therefore it is the desired interpolation formula. Note that Eq. (4) has the same formal aspect of classical interpolation formulas used in FE methods, with the functions $F_m(\boldsymbol{r})$ playing the role of FE shape functions.

As shown by the numerical results of Caruthers et al.,[2] this interpolation formula behaves very well in the reconstruction of acoustic fields, being able to reconstruct an acoustic field with only 2–3 points per wave. It therefore constitutes a solid base for the development of the discretization technique for acoustic problems that we present in this work. Although the interpolation formula is similar to that of Caruthers et al.,[2,3] our approach is quite different from theirs.

Discretization of Helmholtz Equation

Once the local interpolation formula has been constructed, it is possible to apply it to the discretization of the Helmholtz equation. The first step is to obtain a local derivation scheme that allows expression of the derivatives of the potential in a generic point $\boldsymbol{r}$ in terms of the values ϕ_m. This can be obtained easily with a simple derivation of the shape function F; for example, the first derivative in the x direction is given by

$$\frac{\partial}{\partial x}[\phi(\boldsymbol{r})] = \sum_{m=1}^{M} F_{mX}(\boldsymbol{r})\phi_m \tag{6}$$

where

$$F_{mX}(\boldsymbol{r}) = \sum_{n=1}^{N} G^{+}_{nm} \frac{\partial}{\partial x}\left[G_o\left(\boldsymbol{r}, \boldsymbol{r}^s_n\right)\right] \tag{7}$$

and analogous expressions can be obtained for the other first- and second-order derivatives.

Consider now a generic three-dimensional domain D in which the potential ϕ is governed by the Helmholtz equation with the associated boundary conditions on ∂D:

$$\nabla^2\phi + k^2\phi = 0 \qquad (\boldsymbol{r} \in D), \qquad BC(\phi) = b \qquad (\boldsymbol{r} \in \partial D) \tag{8}$$

Once Eqs. (4) and (6) are available, several strategies can be applied to discretize Eqs. (8), ranging from simple collocation methods up to different versions of the weighted residual approach. In the current formulation, we adopt the collocation method because of its simplicity; further studies have to be conducted to assess the advantages of more sophisticated methods. We therefore impose the verification of the Helmholtz equation for all of the internal nodes of the discretization domain D, obtaining the following equations:

$$\sum_{m=1}^{M(i)} A^i_m \phi^i_m = 0 \qquad (i = 1, N_d) \tag{9}$$

and, using Eqs. (4) and (6), it is possible to write

$$A^i_m = F^i_{mXX} + F^i_{mYY} + F^i_{mZZ} + k^2 F^i_m \tag{10}$$

where

$$F^i_m = \sum_{n=1}^{N} G^{+}_{nm} G_o(\bar{r}_i, \bar{r}_n), \qquad F^i_{mXX} = \sum_{n=1}^{N} G^{+}_{nm} \frac{\partial^2}{\partial x^2}[G_o(\bar{r}_i, \bar{r}_n)] \tag{11}$$

The expressions for the other derivatives are analogous.

It is worthwhile to mention that the stencil nodes $M(i)$ associated with each collocation point i define the nodes that can affect the potential derivatives at node i. The interesting aspect of the proposed formulation is that the definition of each stencil is completely arbitrary for what concerns both the number of nodes and their position with respect to the collocation node i. Clearly, numerical considerations pose some limitations, but this aspect has a big advantage with respect to FD methods. In the current implementation the nodes of the stencil are defined as the nodes directly connected to node i, but higher-order formulations can be obtained with very few modifications to the code, considering a second layer of nodes.

A similar discretization approach also can be used for the boundary conditions (see the Appendix) and, therefore, at this point, most of the work seems to be completed. However, a deeper analysis shows a big problem that could make this method completely useless if some corrective action is not introduced. The source of the problem is due to the properties of the shape functions F, which are designed so that any function described with them automatically satisfies the Helmholtz equation independently of the values of ϕ_m. This makes all of the coefficients A^i_m identically null because they are obtained by derivation of the shape functions F. In other words, the discretized Eqs. (9) are all identities because the verification of the Helmholtz equation already has been ensured with the definition of the shape functions F. As a first step in the description of the solution that we adopt, it is useful to introduce the method proposed by Caruthers et al.[2]

Consider Eq. (4), written for the ith node:

$$\phi(\boldsymbol{r}_i) = \phi_i = \sum_{m=1}^{M(i)} F^i_m \phi^i_m \tag{12}$$

Clearly, if node i is considered to be within the mth nodes that constitute its stencil (e.g., if it is the first node of the stencil), then Eq. (12) is an identity because all of the coefficients F^i_m are zero except F^i_1, which is equal to 1.

An alternative approach, proposed by Caruthers et al.,[2] is to exclude node i from the stencil when evaluating the coefficients F^i_m. In this case, Eq. (12) is no longer an identity and can be interpreted as a compatibility condition that relates the value ϕ_i of the potential at node i to the values ϕ^i_m of the potential at the nodes of the stencil of i. It is fundamental to recognize that in this approach the local verification of the Helmholtz equation is ensured only by the shape function, and the discretized Eqs. (12) simply impose a compatibility condition among each node and the nodes of its stencil but does not discretize the Helmholtz equation itself. The limits of this approach appear when we want to consider equations different from the simple Helmholtz equation, as happens when we describe sound propagation in nonuniform mediums. In this case the Green's function of the governing equation is no longer available, and therefore it is no longer possible to build a shape function F that locally satisfies the governing equation. A possible remedy proposed by Caruthers et al.[4] is to try to obtain an approximate Green's function using a wave expansion technique, but this is feasible only for small nonuniformities. Besides, the wave expansion technique necessarily introduces some degree of inaccuracy in the definition of the shape functions and, because in the approach of Caruthers et al. the verification of the governing equation is ensured only by the appropriate definition of the shape functions, the formulation does not seem to be robust enough.

A completely different approach is proposed here. Instead of rejecting Eq. (9), our strategy is to try to modify the coefficients A^i_m to prevent them from being identically null. As we have seen, the coefficients A^i_m are zero because any function described with the local interpolation formula (4) is an exact solution of the Helmholtz equation, and therefore its Helmholtz operator automatically will be zero. Clearly, if we replace F with a different shape function, the problem disappears, but on the other hand we want to keep the new shape function as close as possible to the previous one to preserve its efficiency in modeling acoustic phenomena. Thus, there are two opposite tendencies that drive us in the definition of the new shape functions: The potential described by means of the local interpolation formula does not have to be an exact solution of the Helmholtz equation, but we do not want to move too far away in order to maintain a good description of wave propagation.

For clarity, we first explain our solution in two dimensions and then we consider the three-dimensional case. Suppose therefore that we want to solve the two-dimensional Helmholtz equation on a two-dimensional domain. If we distribute the fictitious sources on a circle and consider in Eq. (1) the two-dimensional Green's function, we come back to the same problem and again obtain all A^i_m equal to zero. However, a simple remedy can be obtained if we distribute the fictitious sources on a sphere and use in Eq. (1) the three-dimensional Green's function. The interpolation formula obtained is in fact an exact solution of the three-dimensional Helmholtz equation, but, because we are discretizing the two-dimensional equation, the A^i_m coefficients will be different from zero. On the other hand, the three-dimensional Green's function has a strong relationship to the physics of wave phenomena, even if we are considering the two-dimensional case, and so, it is reasonable to expect that the interpolation formula will still preserve its accuracy. In effect, numerical tests have been executed on simple two-dimensional test cases, showing that, with the above formulation, good results can be obtained with discretization as coarse as 2–3 points per wavelength. Because the method works fine for the two-dimensional case, it is reasonable to try to use it as a starting point for developing the full three-dimensional formulation. A rather natural extension can be obtained if we introduce a fictitious fourth spatial dimension, interpreting the vectors $\boldsymbol{r}, \boldsymbol{r}^s, \boldsymbol{r}^p$ that appear in G_o and in Eqs. (1) and (2) as four-dimensional vectors and distributing the N sources on a four-dimensional hypersphere.

To preserve the complete parallelism with the two-dimensional case, we should use in Eq. (2) the Green's function of the four-dimensional Helmholtz equation. However, in the current formulation, we use the three-dimensional Green's function because of its simple analytic expression. Clearly, further studies are required to assess whether the use of the four-dimensional Green's function can provide any further advantage.

Some Numerical Results

To analyze the capabilities of the proposed Green's function discretization (GFD) method, we modeled some three-dimensional problems whose theoretical solutions are known. Two cases are considered. In both, the computational domain is a cube of unitary length, but different boundary conditions are imposed on the cube faces. The first problem (Fig. 2) simulates sound propagation in a uniform medium and is referred to as the radiation case. A source is placed on a diagonal of the cube (outside the computational domain), and a Dirichlet condition, obtained from the source itself, is imposed on the three faces visible from the source. A radiation condition is imposed on the other faces. The GFD method then is used to compute the potential inside the cube, which is compared with the known solution produced by the source. The second problem, referred to as the scattering case, simulates sound propagation in the presence of a rigid plain wall with the source again placed on the diagonal of the cube (Fig. 3). One face of the cube ($x = 0$; the dark shaded part of the figure) is placed on the rigid wall and a tangency condition is applied; the opposite face (the light shaded one) is modeled with a scattering condition (see Appendix). The other faces (white) are described with a Dirichlet condition obtained from the exact theoretical solution produced by the source in the presence of the rigid wall.

Numerical results are presented for regular, randomly, and systematically distorted meshes, as well as for combinations of random and systematic distortions. A few results are presented as surface plots of the potential on a plane section of the cube, but most of the results are presented as convergence histories in terms of the source wave number.

The first result reported in Fig. 4 concerns the radiation problem for a discretization of $16 \times 16 \times 16$ nodes with a wave number $k = 30$, corresponding to about 4 points per period in the case of propagation along the edges of the stencil. The surface plot of the real and imaginary parts of the potential distribution (continuous line) is compared with the theoretical solution (dots) for a plane section of the cube. In spite of the reduced number of points per period, it is possible to see that the two solutions compare fairly well. The second case, reported in Fig. 5, concerns a scattering problem with the same discretization and with a wave number $k = 20$. Similar accuracy also can be obtained for higher values of the wave number, but, because of the complex behavior of the field, they cannot be visualized well. The same cases are considered in Fig. 6, which compares the convergence behavior of the radiation and scattering test cases as a function of the wave number for a regular Cartesian mesh of $6 \times 6 \times 6$ nodes. In particular, the abscissa reports the value of the product $k\Delta$, with k being the wave number and Δ the distance among the nodes in the discretization stencil. The right and left ordinates give, respectively, the normalized amplitude and phase errors, defined as

$$\text{Amp err} = \sqrt{\frac{\sum_{i=1}^{N_t} \left[|\phi_i| - \left|\phi_i^{theor}\right| \right]^2}{\sum_{i=1}^{N_t} \left|\phi_i^{theor}\right|^2}}$$

$$\text{Phase err} = \frac{\sum_{i=1}^{N_t} \angle\phi_i - \angle\phi_i^{theor}}{\sum_{i=1}^{N_t} \left(\angle\phi_i^{theor}\right)} \tag{13}$$

Note that a value $k\Delta = \pi$ corresponds to a discretization with 3 points per period in the case of a rectangular stencil and waves propagating along the edges. From the figures, it appears that the solution is accurate enough also for high values of $k\Delta$. As an example, for $k\Delta \approx 2.5$, the overall error is below 10%. In Figs. 7–9, the radiation test case is considered using various kinds of irregular meshes. In Fig. 7, angular distortions of 20, 30, and 40 deg are applied to the Cartesian regular mesh along both the x and y axes. In Fig. 8, random perturbations of 0.1Δ, 0.2Δ, and 0.3Δ applied to x, y, and z coordinates of all internal nodes are considered. Finally, in Fig. 9, combinations of random perturbations and angular distortions are analyzed. As it is possible to see, the method seems to be extremely robust in terms of both random and systematic stencil irregularities because accuracy is good except when distortions are

faces	Boundary Condition
$x = 0$	Dirichlet
$x = 1$	Radiation
$y = 0$	Dirichlet
$y = 1$	Radiation
$z = 0$	Dirichlet
$z = 1$	Radiation
Source	(−6.0, −6.0, −6.0)

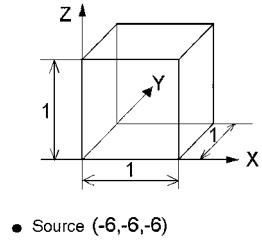

Fig. 2 Schematic view of radiation test case.

faces	Boundary Condition
$x = 0$	Tangency
$x = 1$	Scattering
$y = 0$	Dirichlet
$y = 1$	Dirichlet
$z = 0$	Dirichlet
$z = 1$	Dirichlet
Source	(4.0, 4.0, 4.0)

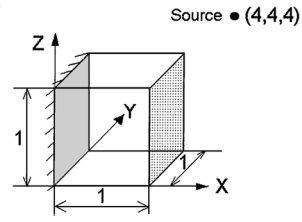

Fig. 3 Schematic view of scattering test case.

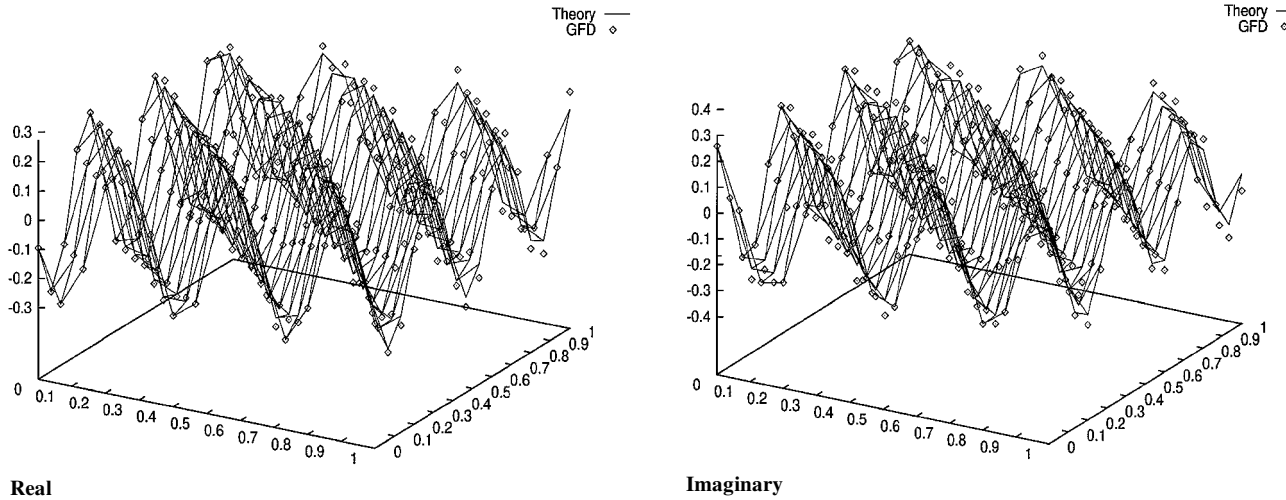

Fig. 4 Radiation case (acoustic potential on a plane at $h \approx 0.26$, $16 \times 16 \times 16$ nodes, $k = 30$).

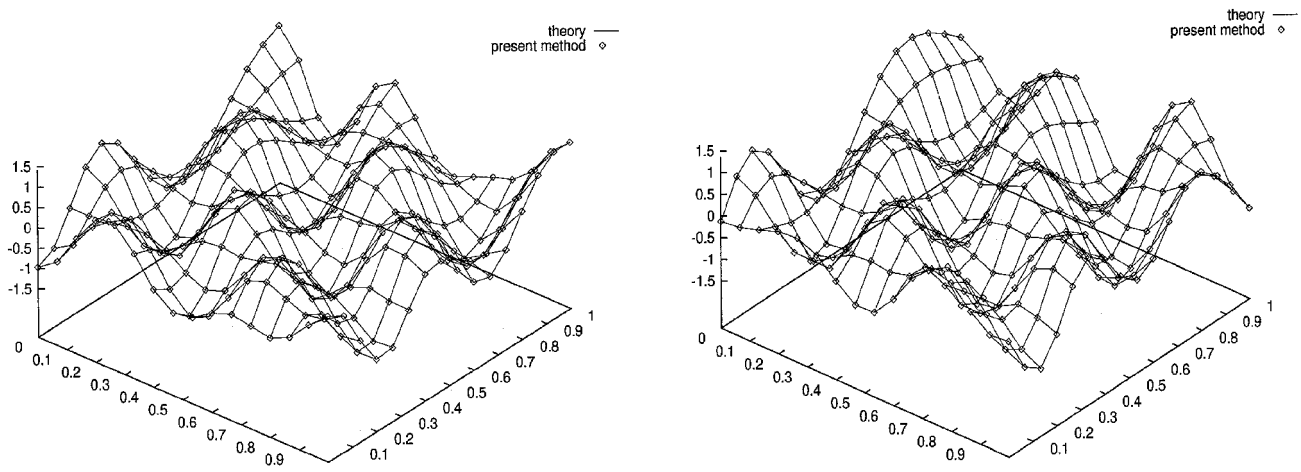

Fig. 5 Scattering case (acoustic potential on a plane at $h \approx 0.53$, $16 \times 16 \times 16$ nodes, $k = 20$).

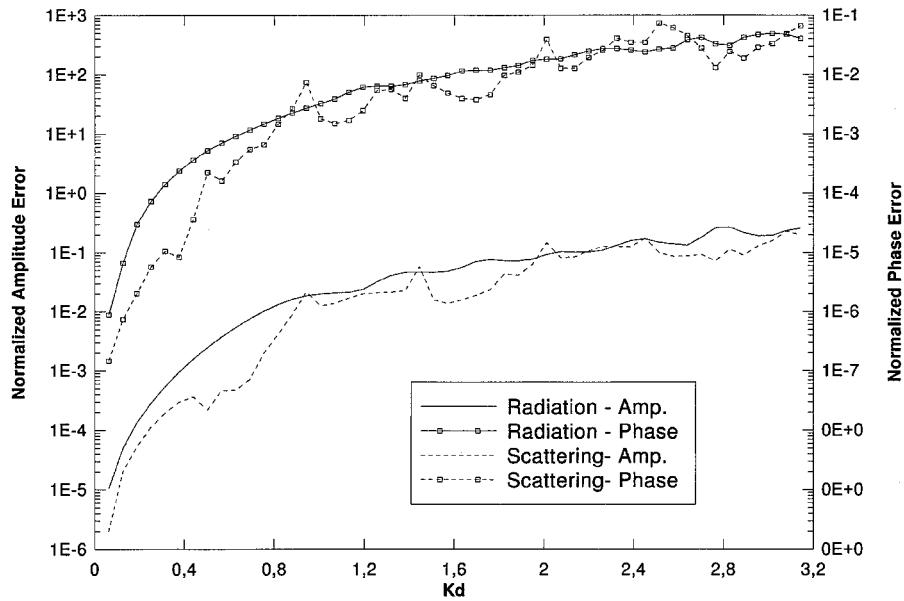

Fig. 6 Radiation and scattering test cases with Cartesian regular mesh, $6 \times 6 \times 6$ nodes: Comparison of normalized amplitude and phase errors in terms of source frequency.

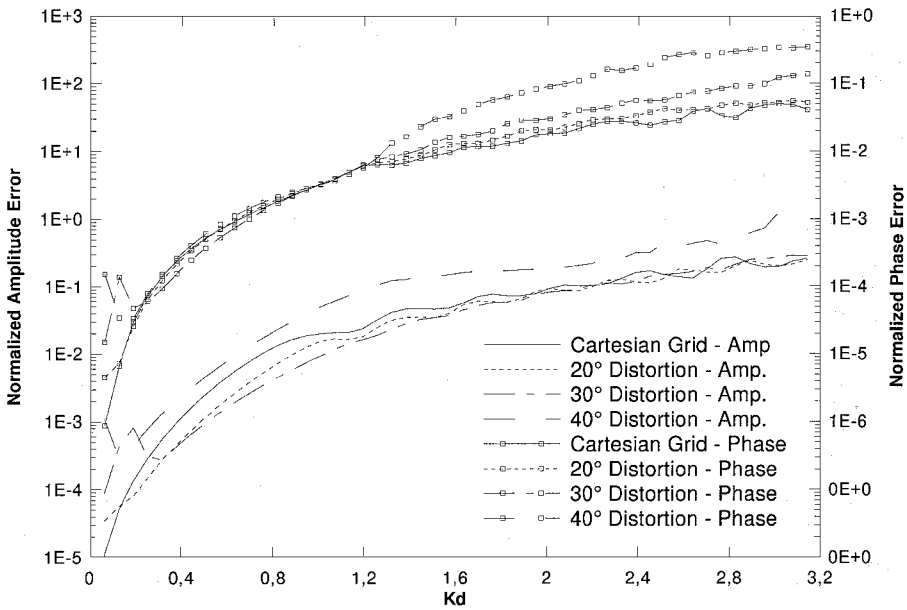

Fig. 7 Radiation case: Comparison of regular Cartesian mesh with angular distorted grids (10, 20, 30, and 40 deg); normalized amplitude and phase errors are compared in terms of source frequency.

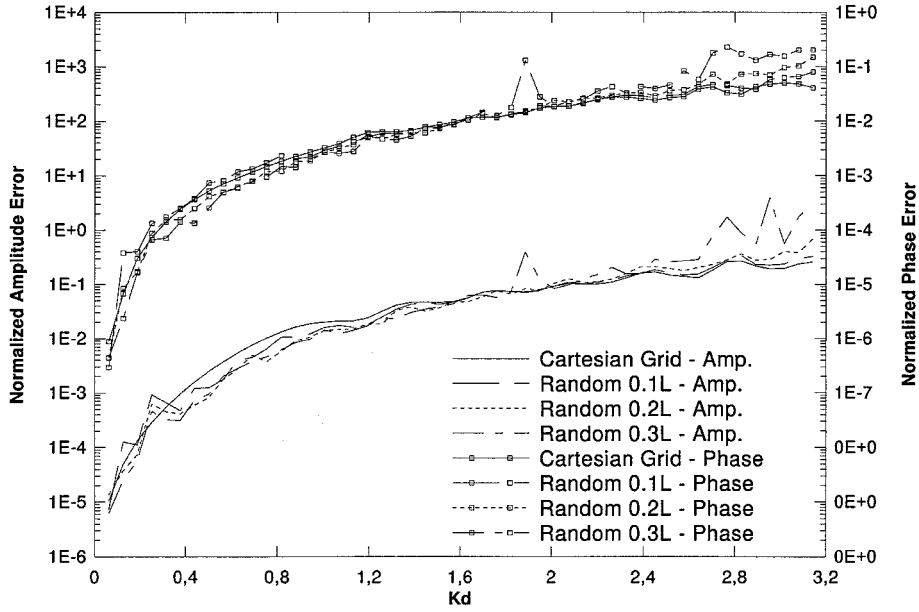

Fig. 8 Radiation case: Comparison of regular Cartesian mesh with randomly distorted grids (10, 20, and 30%); normalized amplitude and phase errors are compared in terms of source frequency.

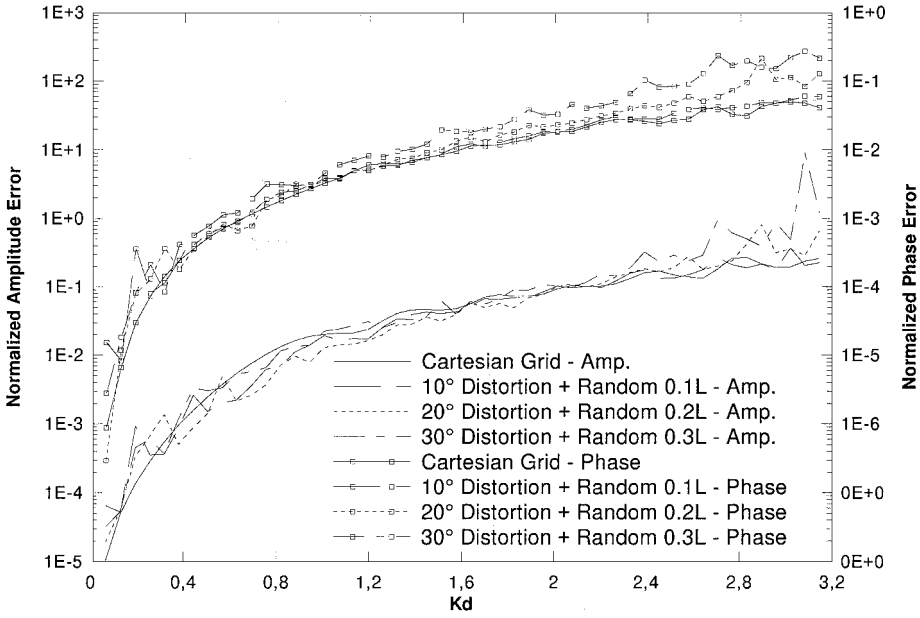

Fig. 9 Radiation case: Comparison of regular Cartesian mesh with combination of random and systematic distortions; normalized amplitude and phase errors are compared in terms of source frequency.

very high. As a last result, a similar analysis is executed in Fig. 10 for the scattering test case, comparing the regular mesh result with one obtained with a random perturbed mesh of 0.2Δ. In this case, good results are obtained with the random mesh except for high $k\Delta$ values. Remember, however, that the tangency condition applied in this test case is inherently less robust than that of the boundary conditions applied in the radiation test case.

Discretization Scheme for Nonuniform Flows

Once the formulation has been developed and tested for the linear Helmholtz equation, it is rather simple to extend it to more complex cases. Consider, for example, the propagation of small acoustic disturbances in a known nonuniform aerodynamic flowfield. The propagation of a small harmonic acoustic disturbance in a nonuniform irrotational flow can be described by the following partial differential equation (see, e.g., Refs. 6 and 7):

$$\begin{aligned}\left\{1+[(\gamma-1)/2]\left(M_\infty^2-M^2\right)\right\}\nabla^2\phi+\mathrm{i}2k\bar{M}\cdot\nabla\phi\\ -\nabla(M^2/2)\cdot\nabla\phi-\bar{M}\cdot\nabla(\bar{M}\cdot\nabla\phi)-(\gamma-1)(\nabla\cdot\bar{M})\bar{M}\cdot\nabla\phi\\ +\mathrm{i}(\gamma-1)k(\nabla\cdot\bar{M})\phi+k^2\phi=0\end{aligned}\tag{14}$$

Equation (14) results from linearizing the nonlinear full potential equation around a mean steady aerodynamic flowfield and assuming a harmonic velocity potential in the form $\phi_{ac}=\phi e^{-\mathrm{i}\omega t}$.

A first approach could be simply to evaluate the derivation coefficients (F^i_{mX}, F^i_{mXX}, F^i_{mXY}, ...) required for the discretization of Eq. (14) using the same shape functions F developed for the Helmholtz equation. With this approach we locally describe the acoustic potential as a solution of the linear Helmholtz equation, but because we effectively discretize Eq. (14) we can still get the correct solution. This is one of the advantages of the new formulation over the one proposed by Caruthers et al.: it allows correct solutions to be

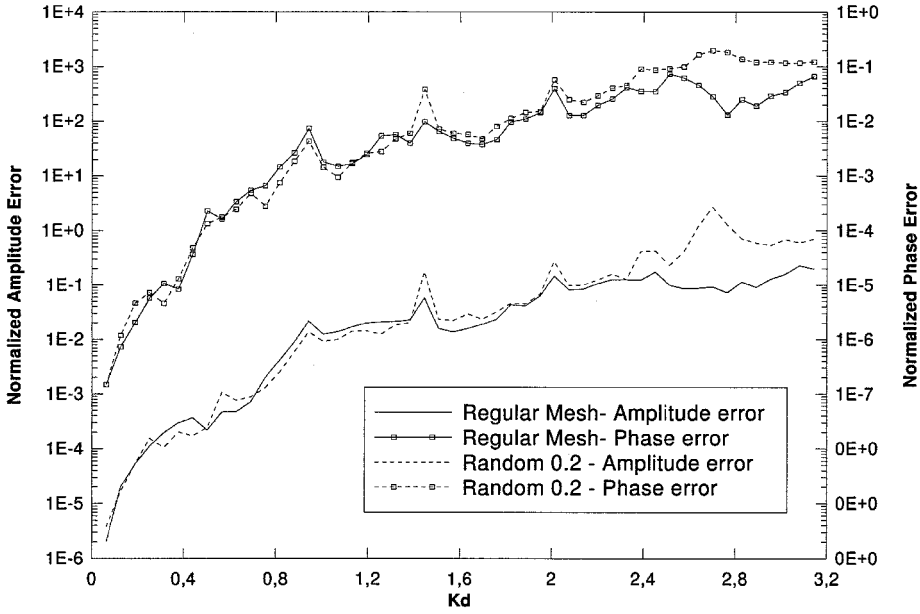

Fig. 10 Scattering case: Comparison of regular Cartesian mesh with randomly distorted grids, 6 × 6 × 6 nodes; normalized amplitude and phase errors are compared in terms of source frequency.

obtained even if the interpolation formula is based on a incorrect Green's function. Even if this simple approach works reasonably well, it is clear that improvements in efficiency can be obtained with a better choice of the interpolation function. Use of the Green's function of the linear Helmholtz equation during the derivation of the shape function F is equivalent to assuming that the fluid is at rest. A natural improvement therefore can be obtained if one assumes that the fluid is locally in uniform motion, adopting the convective Green's function G_c instead of G_o during the derivation of the shape functions F. The new shape function therefore can be written as

$$F_m(\bar{r}) = \sum_{n=1}^{N} G^{c+}_{nm} G_c\big(\bar{r}, \bar{r}^s_n; \bar{M}(\bar{r})\big), \qquad G^c_{nm} = G_c\big(\bar{r}^p_m, \bar{r}^s_n; \bar{M}(\bar{r})\big) \tag{15}$$

The discretized formulation of Eq. (14) can be written in form (9), where the coefficients A^i_m are given by

$$\begin{aligned} A^i_m = {} & \big[1 - \mathcal{A} - M_x^2\big]_i F^i_{mXX} + \big[1 - \mathcal{A} - M_y^2\big]_i F^i_{mYY} \\ & + \big[1 - \mathcal{A} - M_z^2\big]_i F^i_{mZZ} - 2\big[M_x M_y\big]_i F^i_{mXY} \\ & - 2\big[M_x M_z\big]_i F^i_{mXZ} - 2\big[M_y M_z\big]_i F^i_{mYZ} \\ & + \big[\mathrm{i}2kM_x - \mathcal{B}_x - \mathcal{C}M_x\big]_i F^i_{mX} + \big[\mathrm{i}2kM_y - \mathcal{B}_y - \mathcal{C}M_y\big]_i F^i_{mY} \\ & + \big[\mathrm{i}2kM_z - \mathcal{B}_z - \mathcal{C}M_z\big]_i F^i_{mZ} + \big[k^2 + \mathrm{i}k\mathcal{C}\big]_i F^i_m \end{aligned} \tag{16}$$

with

$$\mathcal{A} = \frac{\gamma - 1}{2}\big(M^2 - M_\infty^2\big) \tag{17}$$

$$\mathcal{B}_x = 2\left(M_x \frac{\partial M_x}{\partial x} + M_y \frac{\partial M_y}{\partial x} + M_z \frac{\partial M_z}{\partial x}\right)$$

$$\mathcal{B}_y = 2\left(M_x \frac{\partial M_x}{\partial y} + M_y \frac{\partial M_y}{\partial y} + M_z \frac{\partial M_z}{\partial y}\right) \tag{18}$$

$$\mathcal{B}_z = 2\left(M_x \frac{\partial M_x}{\partial z} + M_y \frac{\partial M_y}{\partial z} + M_z \frac{\partial M_z}{\partial z}\right)$$

$$\mathcal{C} = (\gamma - 1)\left(\frac{\partial M_x}{\partial x} + \frac{\partial M_y}{\partial y} + \frac{\partial M_z}{\partial z}\right) \tag{19}$$

Numerical Results for Nonuniform Flows

Before showing nonuniform flow calculations, the radiation test case previously described was analyzed by introducing a uniform aerodynamic mean flow corresponding to a Mach number of 0.3 in the y direction. The comparison between our formulation and that of Caruthers et al.[2,3] is very instructive for this case. Figure 11 reports the results for the two approaches, and for each formulation, the shape functions obtained with both the convective and nonconvective Green's functions are considered. As can be seen, the two formulations provide almost identical results when the convective Green's function is used, but our approach is more efficient when the nonconvective Green's function is used. In the test case considered, the convective Green's function corresponds to the exact Green's function of the problem to be solved and so it is reasonable to expect that the formulation of Caruthers et al. works fine, but when a different Green's function is adopted our method still maintains a good accuracy, but the method proposed by Caruthers et al.[2,3] is less accurate. This fact is an important indication of the capabilities of the method in the case of true nonuniform flows, where the effective Green's function is not known.

A difficulty in the analysis of test cases for three-dimensional problems in nonuniform flows is given by the few results available that can be used for comparison. One set of theoretical results was given by Taylor[8] for a pulsating or juddering sphere placed in a nonuniform flow produced by the sphere itself when invested by a flow at low Mach number. A sphere of unitary radius $a = 1$, pulsating with a wave number $k = 1$, and invested by an asymptotic flow with $M = 0.1$ in the x direction is considered. In this case the results provided by Taylor[8] can be considered correct because the assumptions on which the solution is based can be considered to be verified (M and Mka both small). Even if the problem presents an axial symmetry, it is treated here as a fully three-dimensional problem; the computational grid is obtained starting from a surface pannelization of the sphere with 1280 triangular panels, and the volume mesh is obtained by introducing 11 spherical layers in the region between $r = 1$ (the surface of the sphere) and $r = 7$ (the outer part of the computational domain), for a total of 7062 nodes and 12,800 volume elements. For the frequency to be analyzed ($k = 1$), this discretization corresponds to about 6 points per period in the outer portion of the mesh. A tangency condition that correctly describes the pulsation[7,9] is imposed on the sphere surface, and a radiation condition (see Appendix) is imposed on the outer portion of the mesh ($r = 7$). Figure 12 gives the real and imaginary parts of the acoustic potential in the plane $y = 0$ for two different radii ($r = 2$ and 4) as functions of the polar angle θ. As can be seen, in

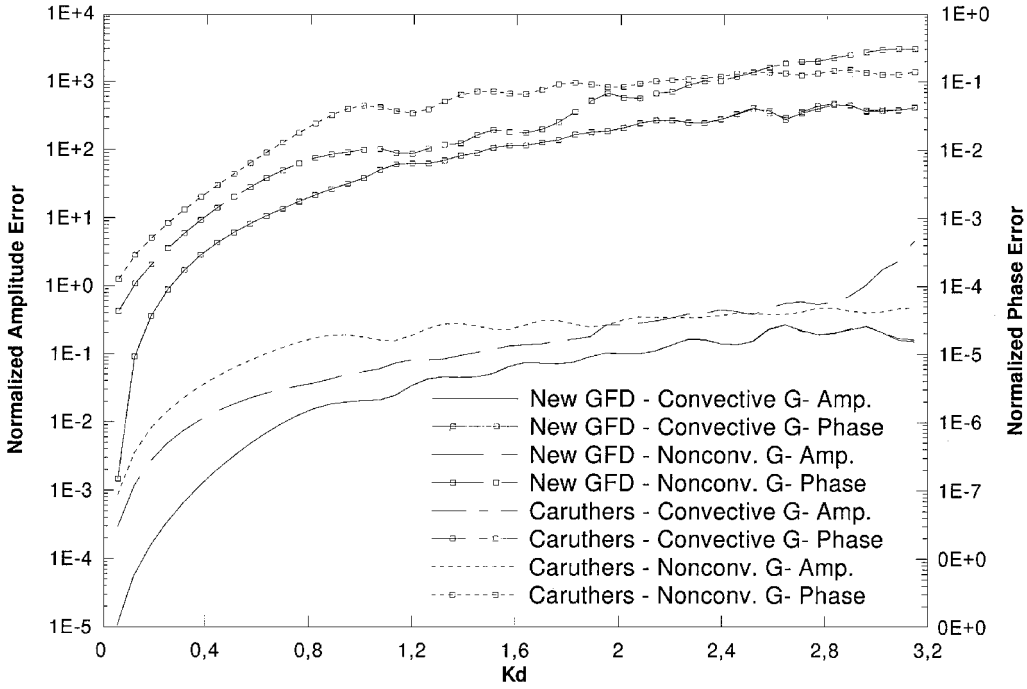

Fig. 11 Comparison of proposed GFD approach with approach of Caruthers et al., using convective and nonconvective Green's functions in radiation test case with uniform flow of $M = 0.3$ in the y direction; normalized amplitude and phase errors are compared in terms of source frequency.

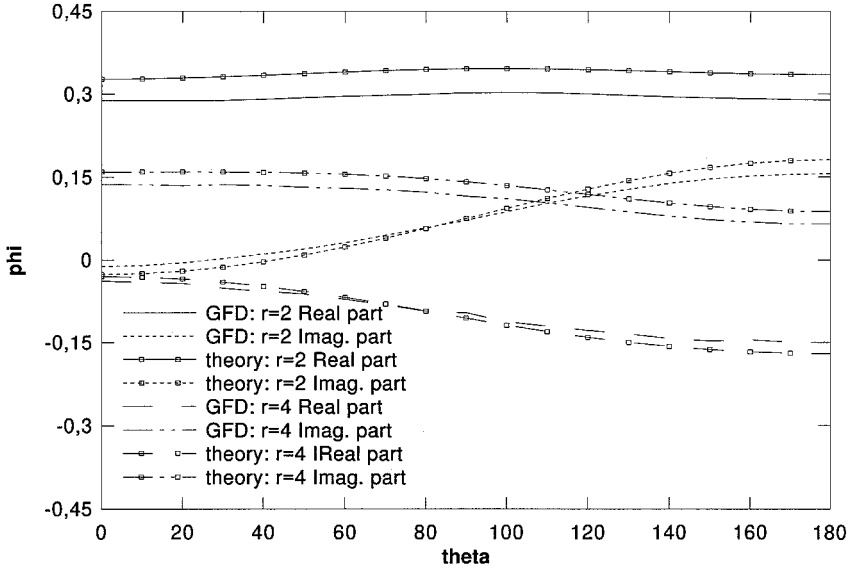

Fig. 12 Pulsating sphere with $M = 0.1$ and $k = 1.0$: Comparison with theoretical results for radii $r = 2$ and 4.

spite of the reduced number of points per period and the reduced outer extension of the mesh, the agreement with theoretical results certainly can be considered satisfactory, and the variation of the potential with the angle θ is well captured. Figure 13 reports the potential on the surface of the sphere for a case with $k = 3.1$ and $M = 0.3$, for which the theoretical results are no longer valid. The comparison therefore is executed with the results of an axisymmetric FE code, the results of which are reported by Astley and Bain.[7] The same number of nodes as the previous case is adopted, but in this case the outer portion of the mesh is placed at $r = 3$, resulting in a minimum of about 4 points per wave. The results in this case are also satisfactory.

As a final example of three-dimensional calculations with nonuniform flows, the sound scattered by a vortex is considered as shown in Fig. 14. The Mach distribution inside the vortex is given by $M(r) = M_1$ for $r < r_1$ and by $M(r) = M_1 r_1 / r$ for $r < r_2$, with $M_1 = 0.5$, $r_1 = 0.01$, and $r_2 = 0.2$. A source, placed at a distance $r = 10$, is used to define the incident potential on the lateral surfaces of the cube, on which a scattering boundary condition is imposed. A regular Cartesian mesh of $(11 \times 11 \times 11)$ nodes was used in the calculations. The contour plot of the amplitude of the acoustic potential within the cube in the plane $z = 0.5$ is reported in Figs. 15 and 16, respectively, for two different values of frequency, $k = 5$ and 7. (The external radius of the vortex r_2 also is reported in the figures.) For these cases, results to be used for comparison were not available to the authors, but the behavior of the fields produced is certainly reasonable.

Analysis of the Formulation

As is evident from the preceding sections, the interesting properties of the proposed scheme arise from the peculiarity of the adopted shape functions, which are designed specifically for the problem to be addressed. As an interesting consequence, two discretization stencils, even if geometrically identical, can have different

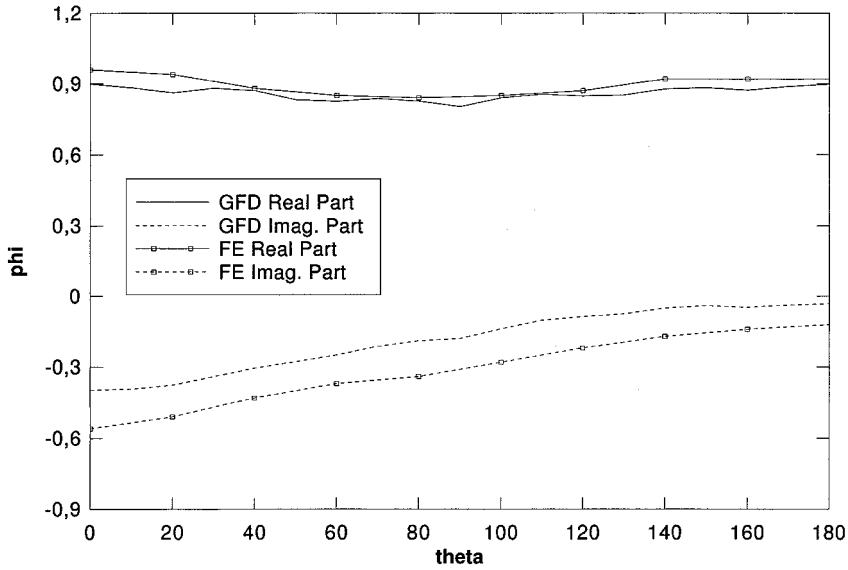

Fig. 13 Pulsating sphere with $M = 0.3$ and $k = 3.1$: Comparison with FE results for surface potential.

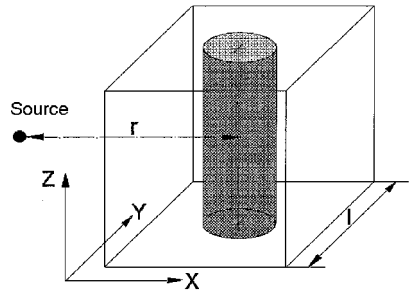

Fig. 14 Schematization of geometry for vortex scattering problem.

discretization coefficients, depending on the local properties of the flow and on the frequency analyzed.

In comparing the new GFD method with classical FE or FD approaches, it is possible to think that its nice properties are obtained by narrowing the space in which the solution is sought. In FE methods, in fact, the shape functions are designed so that, with a sufficiently refined discretization, they can describe a completely generic function. On the other hand, in the GFD approach, the shape functions can describe only a specific set of functions, in particular, the ones that locally satisfy the wave equation for a given frequency. It is clear that, even if the discretization were to be greatly refined, it would be impossible to reconstruct a generic field (e.g., a constant one) that is not a solution of the wave equation for the frequency considered.

Under this point of view, one can consider that the increased accuracy of the proposed method is obtained at the expense of generality, because the formulation works well only for the specific problem for which it is designed. Note that FD methods can be considered, in a certain sense, as a limit case of the GFD approach. The essence of any FD method, when applied to the Helmholtz equation, is the definition of the coefficients of the computational stencil that permit evaluation of the Laplace operator. In an FD approach, these coefficients are independent of the frequency, whereas in the GFD method they depend on the frequency. However, it is possible to evaluate the GFD coefficients forcing $k = 0$ even if the correct value of k clearly is maintained in the discretization of the Helmholtz equation. In this case, one can obtain frequency-independent coefficients that are very similar to classical FD ones. In particular, if we use the classical 7-point three-dimensional stencil typical of second-order-accurate FD discretization on regular Cartesian grids, we obtain exactly the same coefficients of FD, and therefore the method is completely equivalent to an FD method. This fact can be used to compare quantitatively the efficiency of GFD to that of FD methods.

The previously described radiation test case is considered, and a convergence analysis is conducted with the GFD approach and with a modified version of GFD that forces $k = 0$ in the coefficient evaluation (the correct value of k, however, is kept in the discretization) and that is completely equivalent to a second-order FD discretization. To ensure a complete equivalence, a regular Cartesian grid is adopted within the cube and the 7-point computational stencil is used for internal points by both GFD and FD. Also, the boundary nodes are treated in a completely equivalent manner, always using the same stencil in both formulations.

Figure 17 shows a comparison of convergence properties of the two methods (as usual, in terms of normalized amplitude and phase errors), and the great advantages introduced by the GFD method are evident. As can be seen, the order of convergence in the two calculations is similar because it is driven by the number of nodes that constitute the stencil, which is exactly the same for both internal and boundary nodes. On the other hand, GFD is more than one order of magnitude more accurate than FD in all frequency ranges. If we want to compare FD and GFD in terms of computational cost for obtaining a given accuracy, we can see from Fig. 17 that, to get a relative overall error of about 0.01, kd has to be equal to about 0.75 for GFD and 0.16 for FD.

For three-dimensional problems this means that FD requires about 100 times more nodes than required by GFD. On the other hand, evaluation of the GFD coefficients is generally more expensive, but this is greatly compensated by the reduced number of discretization nodes. Another interesting aspect, which can be missed at first view, is the complete topological generality of the proposed approach. With FD schemes the topology of the mesh is limited to a few possibilities (Cartesian, cylindrical, etc.). With FE approaches, the situation is better because the overall mesh can have an arbitrary topology, but in any case it is obtained assembling a large number of elements belonging to a small collection of elements with fixed topology; the FE shape functions are in fact available only for some specific topology of the discretization stencil (cube, tetrahedron, etc.). In the new method, not only can the overall mesh have an arbitrary topology, but each discretization stencil can assume a completely generic topology. The definition of the shape function in a region V_M is based on an arbitrary number of nodes with no specific restriction on their positions within the volume V_M. Clearly, numerical considerations pose practical limits on the relative positions of the nodes, but nevertheless this aspect constitutes an important advantage, which makes implementation of the formulation much easier.

The new approach also can be considered for applications other than aeroacoustic ones. The central idea of the formulation is based on the development of some problem-specific interpolation formula to be used for the discretization. The process for derivation of the interpolation formula is based on knowledge of a Green's function

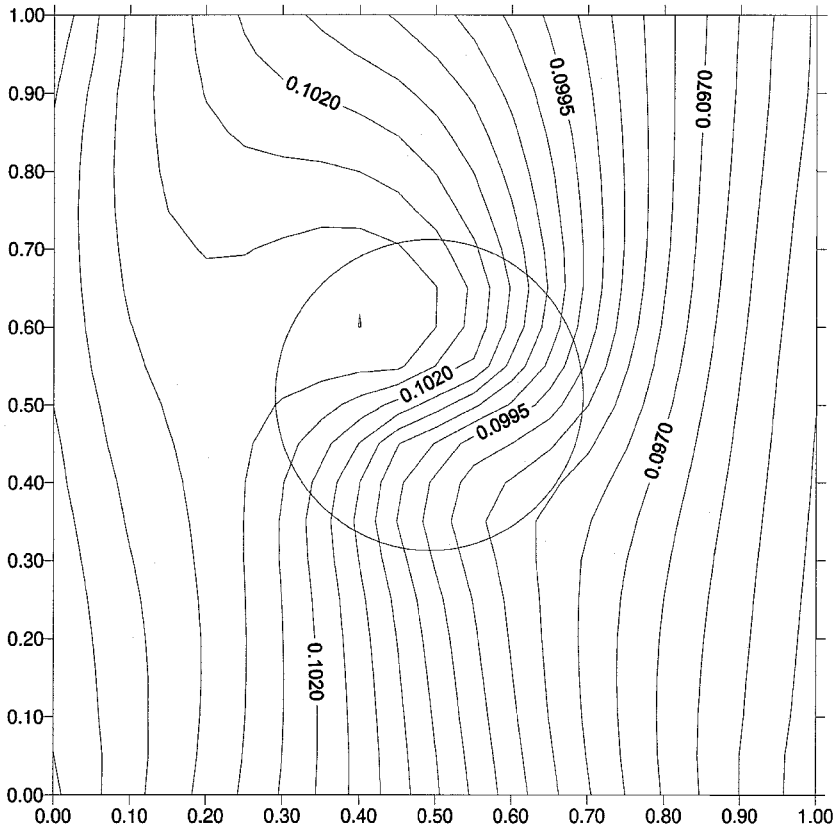

Fig. 15 Sound scattering by vortex ($k = 5$): contour plot of amplitude in the plane $z = 0.5$.

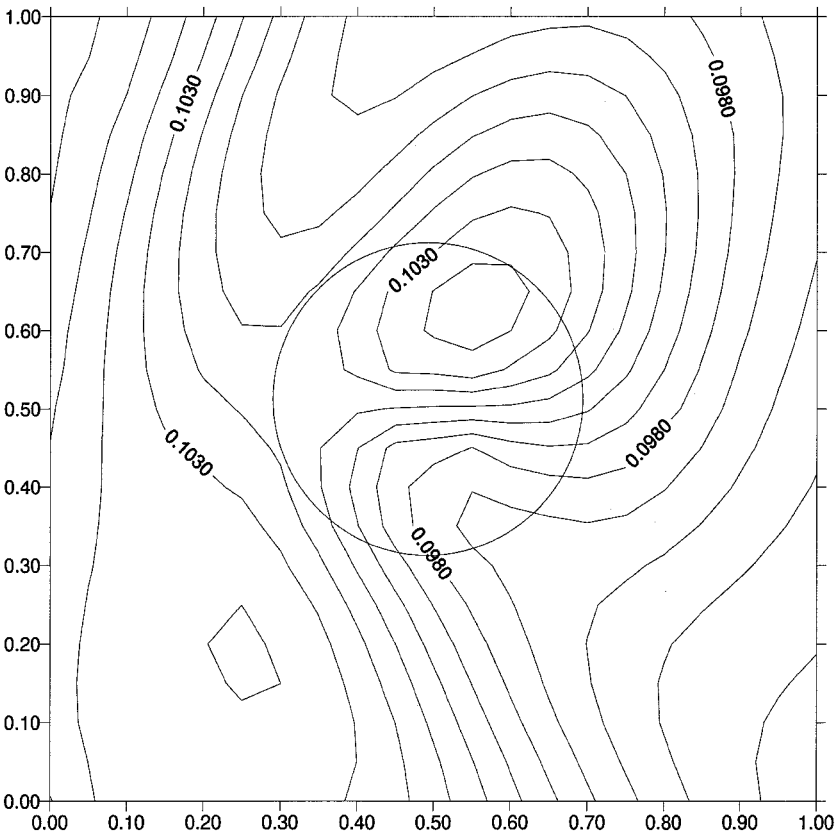

Fig. 16 Sound scattering by vortex ($k = 7$): contour plot of amplitude in the plane $z = 0.5$.

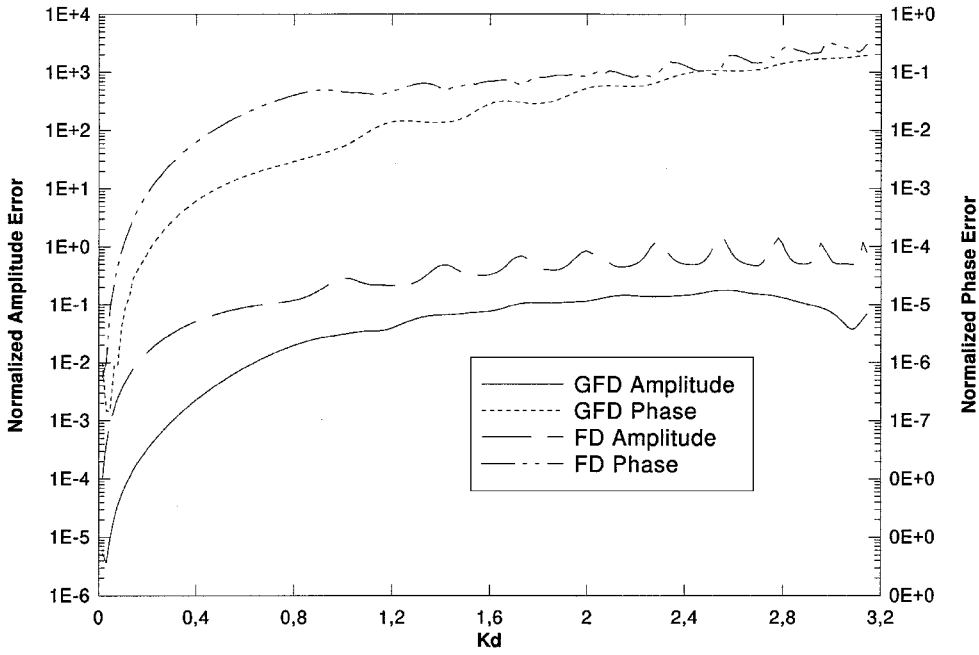

Fig. 17 Comparison of GFD and FD methods based on the same stencil for the radiation test case; normalized amplitude and phase errors are compared in terms of source frequency.

of a simplified equation that is somehow related to the complete equation to be solved. In the analyzed case, the simplified equation, whose Green's function is known, is the convective wave equation, but clearly a number of different problems can be addressed with a methodology such as this.

The method also makes it possibile to model different kinds of boundary conditions efficiently by developing specific shape functions for the desired condition (see Appendix).

Further investigations should be conducted to clarify the advantages of the method as well as its limitations. In particular, it would be interesting to have a full understanding of the implications of the introduction of the fictitious fourth space dimension, and eventually of the use of a four-dimensional Green's function. Other interesting aspects concern the possibility of extending the method to other kinds of equations, and introducing more sophisticated collocation techniques.

A major improvement of the formulation, which is now under investigation, could be the development of an analogous formulation in the time domain, which could permit the method to be applied to fully nonlinear equations.

Conclusions

A new frequency-domain discretization for aeroacoustics problem, which can be applied to the description of small-disturbance propagation in nonuniform flows, is presented. The method permits a good accuracy up to 3–4 points per period in the three-dimensional case with unstructured meshes, and therefore it represents an effective improvement over methods currently available. The scheme has proved to be extremely robust in terms of both systematic and random mesh irregularities, and several numerical results are presented to substantiate the nice properties of the method. From a different perspective the method also can be regarded as an efficient discretization approach for a wide range of partial differential equations.

Appendix: Theoretical and Numerical Aspects of Implementation of Boundary Conditions

Some theoretical and numerical aspects of implementation of boundary conditions in the presence of flow are described. Neglecting the trivial Dirichlect condition and the tangency condition that is well treated by Myers,[9] we focus on radiation and scattering conditions.

Radiation and Scattering Conditions

A radiation condition can be specified at the external boundary of the domain, where a nonreflecting condition for the acoustic disturbances is required. The desired condition may be obtained by generalizing the asymptotic behavior ($r \to \infty$) of some elementary acoustic fields in the presence of flow,[6] obtaining

$$\frac{\partial \phi}{\partial r} - \mathrm{i}k\mathcal{M}\phi = 0 \qquad \mathcal{M} = \frac{-\bar{M}\cdot\bar{r} + \sqrt{(\bar{r}\cdot\bar{M})^2 + \beta^2 r^2}}{r\beta^2} \tag{A1}$$

The coefficient $\mathcal{M}$ takes into account the direction $\bar{r}$ along which the acoustic disturbances leave the computational domain and an eventual presence, at the external boundary, of an aerodynamic uniform flow defined by the Mach vector $\bar{M}$.

A problem of great practical interest, usually known as the scattering problem, is to determine the effect of a body on the acoustic field produced by generic sources. In this case the body is enclosed in the computational domain and the acoustic sources are placed outside. The external boundary of the computational domain therefore has to satisfy the opposite necessities to define the incident wave, and to allow the scattered wave to leave the computational domain without reflections. These two requirements may be synthesized in a single equation referred to as the scattering condition, which is substantially a radiation condition applied only to the reflected component of the potential. Splitting the total acoustic potential in its incident and scattered components ($\phi = \phi_{sc} + \phi_{inc}$), then from Eq. (A1), it follows that

$$\frac{\partial \phi}{\partial r} - \mathrm{i}k\mathcal{M}\phi = \frac{\partial \phi_{inc}}{\partial r} - \mathrm{i}k\mathcal{M}\phi_{inc} \tag{A2}$$

which defines the scattering condition.

Discretized Formulation of the Boundary Conditions

Once the analytical expressions of the boundary conditions are given, it is clearly possible to use the already-derived shape functions F to discretize them using the usual procedure. However, an alternative approach is available that also has the advantage of showing the great flexibility of the proposed methodology. The shape functions F are determined by solving an underdetermined system with the number of unknown N greater than the number of equations M. It is easy to realize that we have a number $(N - M)$ of additive

conditions that we can apply at our discretion to obtain some modified shape functions that satisfy further requirements. For example, following the suggestion of Caruthers et al.,[3] the verification of the tangency condition can be imposed for a certain number of additive points near the collocation node for which the tangency condition has to be imposed. The shape functions obtained can be considered as modified versions of the F functions, specifically designed for an efficient implementation of the tangency condition. Clearly, similar approaches also can be used for the discretization of other kinds of boundary conditions if the normal implementation is not accurate enough.

References

[1]Roe, P. L., "Technical Prospects for Computational Aeroacoustics," DGLR/AIAA Paper 92-02-032, May 1992.

[2]Caruthers, J. E., French, J. C., and Raviprakash, G. K., "Green's Function Discretization for Numerical Solution of the Helmholtz Equation," *Journal of Sound and Vibration*, Vol. 187, No. 4, 1995, pp. 553–568.

[3]Caruthers, J. E., French, J. C., and Raviprakash, G. K., "Recent Developments Concerning a New Discretization Method for the Helmholtz Equation," AIAA Paper 95-117, May 1995.

[4]Caruthers, J. E., Engels, R. C., and Raviprakash, G. K., "A Wave Expansion Computational Method for Discrete Frequency Acoustic Within Inhomogeneous Flows," AIAA Paper 96-1684, May 1996.

[5]Press, W. H., Teukolsky, S. A., Vettering, V. T., and Flannery, B. P., *Numerical Recipes in Fortran, the Art of Scientific Computing*, 2nd ed., Cambridge Univ. Press, New York, 1992, pp. 51–63.

[6]Casalino, D., "Un Metodo Numerico per lo Studio Della Propagazione e Dello Scattering del Suono in Mezzi non Omogenei," Degree Thesis, Aerospace Dept., Turin Polytechnic, Turin, Italy, May 1997.

[7]Astley, R. J., and Bain, J. G., "A Three-Dimensional Boundary Element Scheme for Acoustic Radiation in Low Mach Number Flows," *Journal of Sound and Vibration*, Vol. 109, No. 3, 1986, pp. 445–465.

[8]Taylor, K., "Acoustic Generation by Vibrating Bodies in Homentropic Potential Flow at Low Mach Number," *Journal of Sound and Vibration*, Vol. 65, No. 1, 1979, pp. 125–136.

[9]Myers, M. K., "On the Acoustic Boundary Condition in the Presence of Flow," *Journal of Sound and Vibration*, Vol. 71, No. 3, 1980, pp. 429–434.

S. Glegg
Associate Editor